Space-time structure of the magnetic field of a laser plasma and methods for its enhancement outside the plasma

A. V. Kabashin and P. I. Nikitin
General Physics Institute of Russian Academy of Sciences, Vavilov Street 38, 117942, Moscow, Russia
(Received 14 February 1996; revised manuscript received 16 September 1996)

A considerable enhancement (more than three orders of magnitude) of the magnetic field outside a laser plasma under a large-scale nonuniformity of the experimental configuration has been observed. Some fundamental peculiarities, which indicate the active role of the target in magnetic field generation, have been established. For example, the target topology, the ratio of its dimensions, the conductivity in contact with a plasma ''ionization aureole'' were found to be important factors, that can determine the structure of magnetic field of the laser plasma. [S1063-651X(97)14502-0]

PACS number(s): 51.60.+a

I. INTRODUCTION

The development of space technologies has stimulated an intensive search for methods of wireless transmission of energy and its conversion to an electric one. A promising approach consists of an energy transfer by a laser radiation and subsequent production of laser plasma on a remote target (see, e.g., Ref. [1]). Such plasma is known to be a source of various electromagnetic phenomena. For example, laser plasma can be used for production of a strong pulsed magnetic field in a free space, which is of great interest for many applications. The methods of magnetic field generation outside the laser plasma were studied in Refs. [2–4]. The plasma was initiated between two electrodes of a broken circuit and the plasma induced emf generated a current through a small wire ring between these electrodes. However, this method produces a magnetic field only in a very limited area of space and requires a specially prepared target and an outer circuit that complicates its practical application.

Another method is based upon the utilization of the spontaneous magnetic field of the laser plasma. Numerous papers report the existence of a magnetic field of a megagauss range within the plasma [5] and field up to 1 kOe within a surrounding ''aureole of UV ionization'' ambient gas (see, e.g., Refs. [6,7]). However, the strong magnetic field exists only inside the plasma conductive medium, while the field magnitude outside the plasma and aureole, e.g., behind the target, usually does not exceed 0.1 Oe even under high radiation intensities $I>10^{12}$ W/cm^2. For magnetic field enhancement outside the plasma and aureole, a magnetic dipole moment of plasma blob was produced. It was attained by either passing the laser beam through a peripheral part of a focusing lens [8] or impinging the beam onto an inclined target [9,10]. As shown later, the main factor in these schemes was connected with the asymmetric distribution of the laser intensity $I(x)$ within the irradiation spot on the target surface, that can be produced by different methods [11]. However, the space-time structures of fields outside the plasma observed by different authors were rather contradictory.

In this paper we report the observation of a method of magnetic field ''splash'' from laser plasma connected with a large-scale spatial asymmetry (LSA) of the experimental configuration. This asymmetry of maximal spatial scale was found to surpass all effects connected with small-scale asymmetries [8–11] and determine the distribution of the magnetic field outside the laser plasma. In addition, peculiarities of the magnetic field generation connected with the presence of the target and its properties (topology, ratio of dimensions, conductivity in contact with the ionization aureole) have been established. Earlier we showed that the production of the LSA leads to an electric current along a conductive target [12].

For a better understanding of our mechanism of field generation, this first stage of the experiments was performed in simplified conditions, in which nonlinear effects in laser plasma do not manifest themselves. We used moderate radiation intensities $I\approx 10^9$ W/cm^2 and relatively large targets (30–80 mm long). The observed effect will be much more significant under higher laser intensities $I\sim 10^{15}$ W/cm^2 and ultra short pulse durations, when new mechanisms of generation of electromagnetic phenomena will make a contribution. These investigations are in progress.

II. EXPERIMENTAL TECHNIQUE

The plasma was produced by two successive pulses of a transversely excited atmosphere (TEA) CO_2 laser (20 J, 4 μs) with a variable delay $\tau=1$–2000 μs between them. The radiation was focused onto various targets with an average intensity of $I\cong 10^9$ W/cm^2. The experiments were carried out at different ambient pressures P, but we present the results only for $P\cong 0.1$ Torr, for which an observed field was a maximum. The conductive targets of copper foil and dielectric targets of Teflon were used in the experiments. Target samples were 0.1–2 mm thick with the dimensions of 30–80 mm.

The magnetic field, in different points behind and in front of the target, was detected by fiber magneto-optical sensors based on the Faraday effect in ferrite-garnet films and semimagnetic semiconductors CdMnTe [13,14]. These sensors have a high noise immunity and permit measurements of the magnetic field in the presence of an electric field and under its irradiation by the UV from plasma. The sensors had a sensitivity threshold of 0.3 Oe. The spatial and temporal resolutions were 2 mm and 0.6 ns, respectively. In addition,

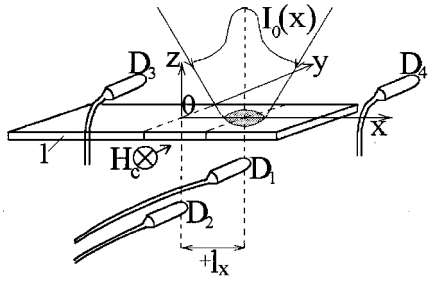

FIG. 1. Experimental scheme. (1)—target, $D_{1\text{-}4}$—sensitive elements of fiber-optical sensors of magnetic field.

in some experiments two-turn inductive coils were used with a diameter of 4 mm.

III. THE MAGNETIC FIELD UNDER PLASMA PRODUCTION ON A CONDUCTIVE TARGET

In the first set of experiments, a laser beam with a symmetric square intensity distribution $I(x)$ over the focal spot was shifted by a distance of $\pm l_x$ from the geometric center of the target to its edges as shown in Fig. 1(a). The focusing spot diameter $d\sim 3$ mm was much less than the target dimensions (33×33 mm^2), so such a shift did not cause the small-scale asymmetry within the plasma itself. However, it resulted in the asymmetric contact of the ionization aureole with the target surface, since at $P=0.1$ Torr ambient gas could be effectively ionized by the plasma UV up to the walls of a vacuum chamber.

The experiments revealed considerable signals of a magnetic field ($H_c=3-4$ Oe) behind the target when the beam was shifted from the target center. The direction of the magnetic field $\vec{H}_c$ shown schematically in Fig. 1 and Fig. 2(a) depended upon the direction of the shift and was defined by a vector product $[\vec{k},\vec{l}_x]$, where $\vec{k}$ is a wave vector of the laser beam and $\vec{l}_x$ is a vector from the target center to the irradiation spot. The duration of typical magnetic field signals [1.5 μs full width at half maximum (FWHM)] correlated with the laser pulse duration, while the maximum coincided with the laser pulse maximum [Fig. 2(b)].

It was found that, as in the case of an air optical breakdown [9,15,16], the plasma ignition by two successive laser pulses in forvacuum also results in a considerable increase of magnetic field amplitudes during the second delayed pulse H_{c2} in the above experimental configuration. In this case the aureole is a strongly ionized plasma produced by the first pulse. However, in contrast to resonantlike dependencies of the magnetic field near the plasma during the second laser pulse $H_{c2}(\tau)$ for atmospheric pressure observed in Refs. [15,16], in our experiments the maximal field behind the target $H_{c2}=(20-40)H_{c1}$ was achieved under a wide range of time delays $\tau=20-200$ μs. Even though the delays were about a few milliseconds, there was no independent action between the first and second pulses, and $H_{c2}=(2-3)H_{c1}$. Such a distinction is probably connected with the longer lifetime of the ionization aureole of the rare ambient gas.

To study the observed effect under conditions of maximal field amplitudes, later we will consider the dependencies only for the second laser pulse delayed for $\tau=100$ μs. Figure

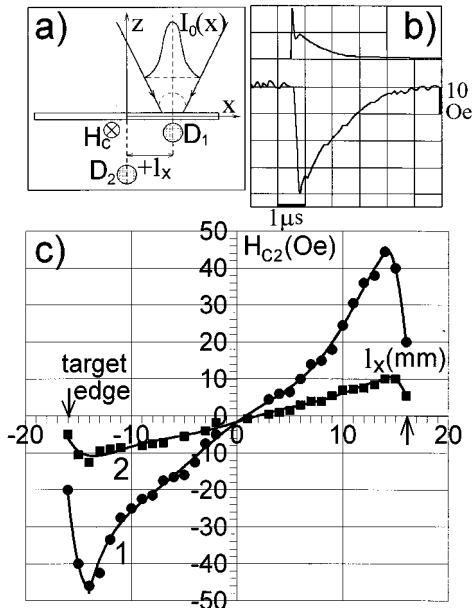

FIG. 2. (a) Experimental scheme, $D_1(l_x,0,-10$ mm), $D_2(0,0,-10$ mm). (b) Temporal shape of laser pulse (upper trace) and typical signal of magnetic field behind a conductive target from fiber-optical sensor under a beam shift from the target center l_x. (c) The amplitude of magnetic field signals H_{c2} behind the conductive target during the second laser pulse as a function of a beam shift from target center l_x. Curve (1) is for the sensor D_1, curve (2)—for D_2.

2(c) presents the dependence of the field amplitudes H_{c2} behind the target on the magnitude of the beam shift l_x. One can see that maximal amplitudes of H_{c2} were reached under the beam shift to the target edges, when the maximal LSA parameter was produced. The amplitudes of the field H_{c2} were 40–50 Oe at a distance of 10 mm from plasma, 15 Oe at a distance of 30 mm, that exceeded the field under plasma production in the target center by more than three orders. The direction of the magnetic field, determined by the initial beam shift, was found to be the same in any point behind the target. The decrease of the magnetic field H_{c2} along the z axis was extrapolated by the function $1/z^{1.8\text{-}2}$. Such a quasidipole decrease is significantly slower than the one during the plasma ignition in the target center. As a result, the magnetic field behind the target could be detected up to distances of about 10–15 cm from plasma.

Experiments with large targets (80×80 mm^2) of different thickness $h=0.1-2$ mm showed that the magnetic field H_{c2} behind the target does not depend on the target thickness and significantly increases only under a certain beam shift to the target edge $l_x>20$ mm. The direction of the field H_{c2} was also the same in any point behind the target and its amplitude was 5–10 Oe at a distance of 30 mm from the plasma. Note that in all experiments the amplitude of the magnetic field component H_{cy} exceeded H_{cx} and H_{cz} by more than an order of magnitude.

A similar magnetic field ''splash'' from the laser plasma was observed in another experimental scheme [Fig. 3(a)]. Here the region of the aureole-target contact was asymmetrically superposed from one of the target edges by a thin layer of dielectric ($\sim$100 mm thick) while the plasma was ignited in the target's geometric center. The direction of the mag-

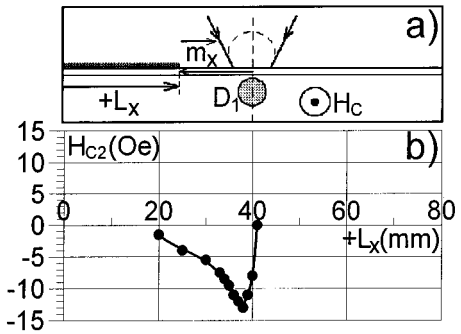

FIG. 3. (a) Experimental scheme, $D_1(0,0,-10$ mm). (b) The amplitude of magnetic field signals H_{c2} behind a conductive target as a function of the position of the dielectric layer on the target surface L_x.

netic field $\vec{H}_c$ shown schematically in Fig. 3(a) also depended upon the direction of the superposition and was defined by a vector product $[\vec{k},\ \vec{m}_x]$, where $\vec{m}_x$ is a vector from the target center to the edge of dielectric. The temporal shape of the signals was similar to the signal presented in Fig. 2(b). Maximal amplitudes of the field H_{c2} were observed under the maximal LSA parameter when all target-aureole contact area was completely superposed from one of the edges [Fig. 3(b)]. However, the field amplitudes diminished when the edge of the dielectric was put into the irradiation spot. This experimental fact differs from the field behavior in Ref. [10], in which the laser beam was shifted along the surface of a complex target consisting of two dielectrics with various densities. Here maximal field amplitudes were detected when the irradiation spot came to the junction of dielectrics. Thus in our conditions the LSA factor is more significant than the factor of nonuniform chemical composition giving rise to a noncollinearity of the gradients of electron temperature ∇T_e and concentration ∇N_e in plasma [10].

Besides, similar field signals behind the target were observed when the upper oxide layer on the target surface contacting with the aureole was asymmetrically removed from one of the edges. The direction of such signals was opposite to the signals observed under the superposition of the same edge by the dielectric layer [Fig. 3(a)].

IV. THE MAGNETIC FIELD UNDER PLASMA PRODUCTION ON A DIELECTRIC TARGET

To understand the mechanism of the magnetic field splash, experiments with a dielectric target of the same dimensions (33×33 mm^2) were carried out. Such a target is not involved in the process of the flowing of plasma currents.

Experiments also revealed considerable signals of a magnetic field behind the target $H_d=1-3$ Oe while the beam was shifted from the target center. The direction of the magnetic field H_d shown schematically in Fig. 4(a) again depended upon the direction of the shift from the center. However, the direction of the vector $\vec{H}_d$ turned out to be the opposite of the field $\vec{H}_c$ observed with the conductive target and was defined by a vector product $-[\vec{k},\vec{l}_x]$. Typical magnetic field signals had the duration of 1.5 μs FWHM, their maximum was delayed for 1–1.5 μs with respect to the maximum of laser

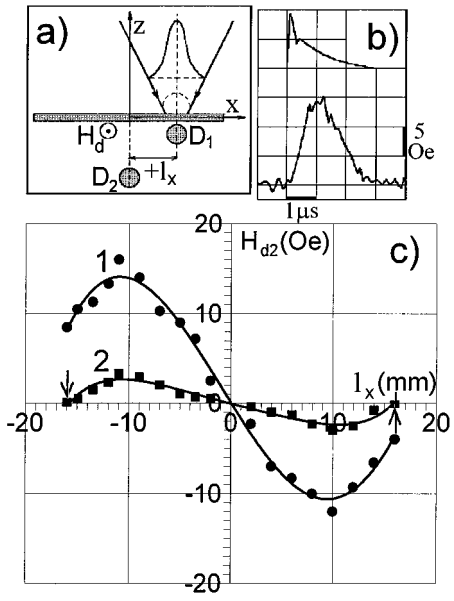

FIG. 4. (a) Experimental scheme. (b) Temporal shape of laser pulse (upper trace) and a typical signal of magnetic field behind a dielectric target under a beam shift from the target center. (c) The amplitude of magnetic field signals H_{d2} behind the dielectric target during the second laser pulse as a function of a beam shift from the target center l_x.

pulse [Fig. 4(b)]. The maximal amplitudes of the magnetic field H_{d2} were achieved under a certain beam shift $l_{x0}\approx11$ mm [Fig. 4(c)] in contrast to the case of conductive target, in which the shift to target edge was the optimal one. The amplitudes of the field H_{d2} were 15–20 Oe at a distance of 10 mm from the plasma, 5 Oe at a distance of 30 mm, that exceeded the field under plasma production in the target center by more than three orders.

V. COMPARATIVE EXPERIMENTS

In this part of the experiments we compared the efficiency of the magnetic field ''splash'' due to the observed effect with such efficiency in the case of an oblique beam incidence onto the target surface [9–11]. As in Refs. [9,10] experiments detected the signals of the magnetic field behind the target while the beam was directed to an inclined target. The direction of the magnetic field depended upon the sign of beam incidence angle α and was the same for the conductive and dielectric targets. Maximal signals of the magnetic field were observed at $\alpha=\pm50$ deg. They reached $\sim$5–10 Oe and $\sim$20 Oe for the conductive and dielectric targets, respectively.

In comparative experiments the laser beam was shifted with respect to the target center to produce an initial large-scale asymmetry. In this position, magnetic field signals were analyzed while the angle of the beam incidence α was varied (Fig. 5). Experiments showed that, under a certain beam shift $l_x>4$ mm from the center of the conductive target, nonuniformity of the largest scale surpasses all effects connected with the small-scale asymmetries caused by the oblique beam incidence. In this case, any variation of the angle α does not change the direction of the magnetic field, originally initiated by the shift (Fig. 5). For the dielectric

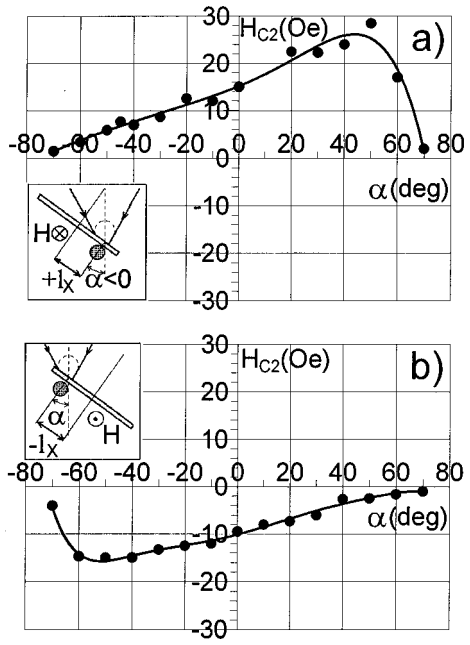

FIG. 5. The amplitude of magnetic field signals H_{c2} behind a conductive target as a function of beam incidence angle α onto the target surface under the production of an initial beam shift from the target center $l_x=8$ mm, $l_x=-8$ mm (b).

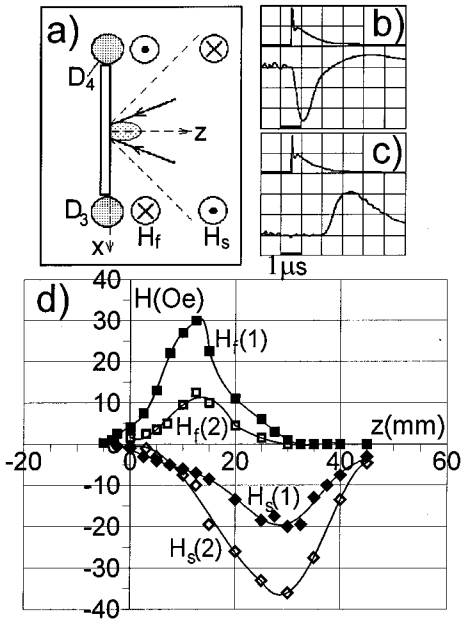

FIG. 6. (a) Experimental scheme, D_3 (25 mm, 0, z), D_4 (-25 mm, 0, z). Temporal shapes of the laser pulse (upper traces) and typical magnetic field signals from fiber-optical sensors in different points: $z=12$ mm (b) and $z=37$ mm (c). (d) The amplitudes of the field components of different polarity H_f and H_s from the sensor D_3 as a function of the z coordinate. Curves (1) are for the conductive target, the curves (2)—for dielectric one.

target, the signals caused by the large- and small-scale asymmetries were comparable.

Allowing for this large-scale factor, it is possible to explain many contradictions in the literature concerning the observed structures of magnetic fields of laser plasma. For example, the authors of Refs. [9,10] detected different directions of magnetic fields in a region behind the target under the same sign of the beam incidence angle. In our opinion, such contradictions can be explained by the fact that these authors did not pay any attention to the location of the irradiation spot with respect to the target center. Such a factor appeared to be more significant than the direction of current rotation due to the radiation pressure [9] or noncompensated current turn in plasma [10] under the oblique beam incidence.

VI. DISTRIBUTION OF MAGNETIC FIELD NEAR LASER PLASMA

To understand the possible reasons for magnetic field ''splash,'' an investigation of magnetic field structure in front of a target was performed. We detected a magnetic field along z axis by fiber-optical sensors D_3 and D_4 as shown in Fig. 6(a) while the plasma was ignited in the center of a target (33×33 mm^2). In the experiments, magnetic field signals during the second laser pulse were analyzed. The temporal shape of these signals was the same as the one during the first pulse but the amplitude was larger by a factor of 20–40.

Experiments showed that the signals from the sensors D_3 and D_4 have the same temporal shape, but different polarity, confirming the toroidal configuration of a magnetic field axially symmetric with respect to the z axis. The signal from each sensor for both the metallic and the dielectric targets consisted of two components of opposite polarity [Figs. 6(b), 6(c)]. The duration of one of them H_f (1–2 μs FWHM) approximately correlated with the laser pulse length [Fig. 6(b)]. The second component H_s (3–5 μs FWHM) was detected with a certain delay 1.5–3 μs with respect to the beginning of the laser pulse [Fig. 6(c)]. The direction of a slower component corresponded to the magnetic field of the electrons moving from the focal spot to the focusing lens [Fig. 6(a)]. The ''fast'' component H_f dominated in a peripheral region in the vicinity of the target, while the ''slow'' component H_s was detected only in front of the target near the axis of laser beam [Fig. 6(d)]. Maximal amplitudes of the H_f component for the dielectric target were less than these components for the conductive one by a factor of 2–2.5, while the amplitudes of H_s were larger by a factor of 1.5.

Note that the authors of Refs. [17] and [18] also indicate the existence of the ''fast'' and the ''slow'' components of the magnetic field of the laser plasma. However, in these papers the ''fast'' component was detected only when a conductive target was used. As a result, ''fast'' component was attributed to an electron emission from the conductive surface. In our experiments, there was no difference between the results for conductive and dielectric targets. This manifests different mechanisms of generation of the observed components.

VII. INFLUENCE OF THE GEOMETRY OF SPREAD OF PLASMA SURFACE CURRENTS ON MAGNETIC FIELD BEHIND A CONDUCTIVE TARGET

In this part of experiments the influence of the target geometric parameters on magnetic field outside the plasma was

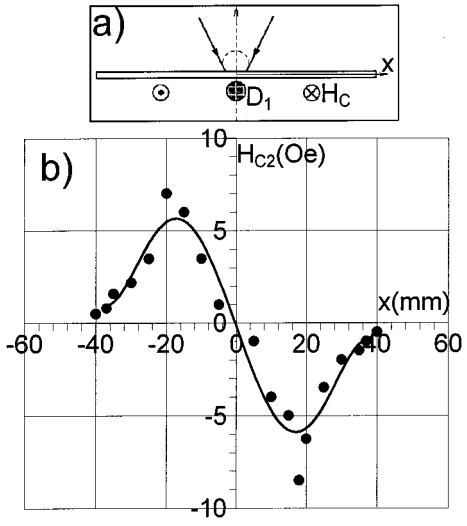

FIG. 7. (a) Experimental scheme, D_1 $(x, 0, -10$ mm). (b) The amplitude of magnetic field signals H_{c2} behind an elongated narrow conductive target (80×20 mm^2) as a function of the x coordinate.

studied. We used targets of the same widths 20 mm, but having different lengths from 20 mm to 80 mm. Sensors D_1 and D_2 detected a magnetic field along the x axis as shown in Fig. 7(a) while the plasma was ignited in the target center.

Experiments showed that the transition from the case of a two-dimensional spread of plasma surface currents (approximately the same length and width of the target) to the anisotropic current flow mainly in the single direction (narrow and long quasi-one-dimensional target) leads to the generation of a magnetic field behind the target. For example, utilization of targets elongated along the x axis resulted in the appearance of the y component of the signal H_{cy}. The direction of such signals was opposite at different sides of the irradiation spot (Fig. 7). Note that the direction of magnetic field signals behind the target was also opposite to the one in front of the target. The most effective generation of the magnetic field behind the target was observed for the 80 mm long target. In this case maximal field amplitudes H_{c2} reached $\sim$10 Oe at $x\approx\pm20$ mm while a magnetic field was not detected directly under the irradiation spot. Note that using the distribution of the magnetic field behind a quasi-one-dimensional target, one can estimate the effective dimensions of a current structure responsible for the magnetic field generation. For rough evaluation these dimensions could be taken as a distance between the maxima of the dependence $H_{c2}(x)$ at different sides of the irradiation spot. In our conditions, such a distance was about 40 mm.

Thus production of the anisotropy in the direction of the plasma current flow over the surface of the conductive target results in the appearance of a magnetic field behind the conductor even under the plasma ignition in the target center.

VIII. DISCUSSION

In our opinion, the observed structure of the magnetic field can be explained by the gradient mechanism, connected with the noncollinearity of the gradients of ∇N_e and ∇T_e in the plasma [6]. Figure 8 shows the distribution of the gradients ∇N_e and ∇T_e, corresponding to this structure. Here two sources of the field and current are distinguished. The first of them is located near the fore plasma front, the second one is near the target surface. Responsible for H_s the source near the forefront may be due to the ∇N_{ez} in the plasma expansion front (∇N_e is maximal in the direction of the main radiation absorption) and the ∇T_e in the transverse directions because of the spatial restriction of the intensity distribution $I(x,y)$ by the spot dimensions. Responsible for H_f, the second source can be due to ∇N_{ez} near the target surface and ∇T_e in the transverse directions. This distribution produces the structure of the field and current, that exists within the conductive medium of plasma and the surrounding ionization aureole. Note that in our experiments amplitudes of the H_f component for the conductive target exceeded this component for the dielectric one. Such a distinction is probably connected with an increase of the ∇N_e near the conductor because of a fast plasma cooling near the metallic surface.

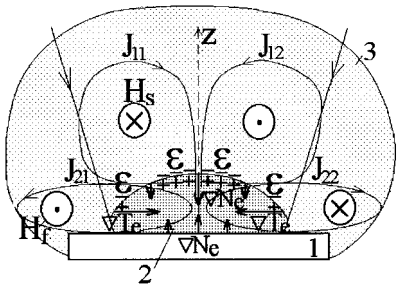

FIG. 8. The qualitative scheme of generation of the current J and magnetic field H of laser plasma constructed on the basis of the experimental data and the results of a computer simulation. (1)—target, (2)—plasma, (3)—ionization aureole.

When a laser beam is shifted to a target edge, the ambient gas near this edge appeared to be more ionized by the plasma UV because all the UV flux in this direction is absorbed only by the gas. For the dielectric target, it results in smaller electric resistances $r_2<r_1$ of the current tubes $J_{22}\sim\varepsilon/r_2$ near the target edge and relative domination of these tubes (Fig. 9). So in spite of the equality of the emfs in the plasma front there arises a resulting large-scale magnetic dipole moment in the system ''plasma-aureole-target,'' which is connected with the tubes J_{22}. This dipole leads to the appearance of a

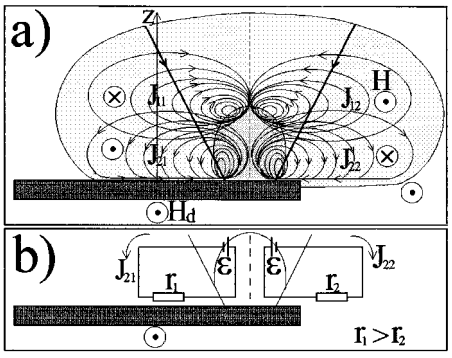

FIG. 9. (a) The qualitative scheme of generation of current J and magnetic field H of laser plasma under the beam shift from the center of a dielectric target. (b) The equivalent electric circuit.

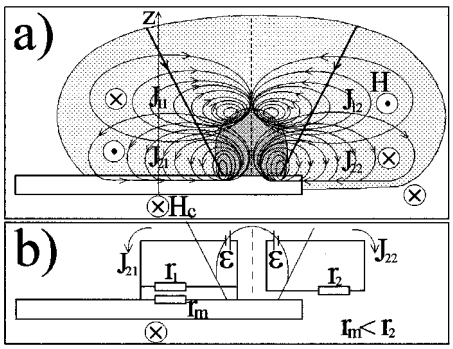

FIG. 10. (a) The qualitative scheme of generation of current J and magnetic field H of laser plasma under the beam shift from the center of a conductive target. (b) The equivalent electric circuit.

magnetic field H_d outside the plasma and aureole, e.g., in a region behind the target.

$$H_d \sim (J_{22} - J_{21}) \sim \varepsilon/r_2 - \varepsilon/r_1 .$$

For the conductive target, this current structure is added by current tubes J_m (Fig. 10), which are closed by the conductive surface of the metal. As these tubes $J_m \sim \varepsilon/r_m$ have very small resistance $r_m (r_m \ll r_1, r_2)$, they became predominant in comparison with J_{22}. This leads to the appearance of a magnetic dipole moment in the system ''plasma-aureole-target'' of the opposite direction. The direction of the field H_c due to such a dipole must also be opposite to the field in the case of dielectric H_d.

$$H_c \sim -(J_{22} - J_m) \sim -[\varepsilon/r_2 - \varepsilon/r_m].$$

IX. CONCLUSIONS

A method of magnetic field generation outside a laser plasma has been found. This method is defined by large-scale nonuniformities of experimental configurations. In particular, a shift of a laser beam from the geometric center of an irradiated target results in a significant (more than 1000 times) field enhancement outside the plasma, e.g., behind the target (magnetic field ''splash''). The similar field enhancement was observed when the ''aureole-target'' contact was asymmetrically superposed by a dielectric layer or an upper oxide layer on the target surface contacting with the aureole was asymmetrically removed. Furthermore, an arbitrary production of the asymmetric contact of the ionization aureole with the target surface leads to the magnetic field ''splash'' from plasma. The structure of the splashed field was established to have a quasidipole configuration while its direction was found to be the opposite for the conductive and dielectric targets. The proposed method of the field generation outside the plasma does not require special target design or any strict conditions of the light focusing.

The LSA factors of the experimental configuration, e.g., the factor of the target shift, were shown to be more important than, e.g., the direction of the current rotation due to the radiation pressure [9] or the noncompensated current turn in plasma [10] arising under the oblique beam incidence or nonuniform chemical composition of the target material. These LSA factors should be allowed for in the interpretation of the experimental results in future. In addition, they can probably explain many contradictions encountered earlier in the literature.

It was established that the plasma production by two successive laser pulses in conditions of forvacuum results in a considerable increase of magnetic field signals during the second delayed pulse H_2 in the above experimental configurations as was observed in Refs. [9,15,16] for the atmospheric ambient pressure. In our experiments the maximal field $H_2 = (15-40)H_1$ was achieved under a wide range of a time delays $\tau = 20-200$ μs. Even when the delays were about a few milliseconds, we did not observe an independent action of the first and second pulses and $H_2 = (2-3)H_1$.

A significant role of different factors connected with the presence of a target and its properties in the process of magnetic field generation of laser plasma has been established. The target topology, the ratio of dimensions (even when they are larger than the focusing spot size by more than 10 times), the conductivity in contact with the ionization aureole can determine the structure of the magnetic field of laser plasma. The production of the anisotropy in the direction of a plasma current flow over the surface of a conductive target (e.g., for a strip target) result in the appearance of magnetic field behind it, even under the plasma ignition in the target geometric center.

The peculiarities of a space-time evolution of the magnetic field of the plasma, produced by CO_2 laser on a solid target, have been established. Two toroidal components of opposite direction evolving in time have been found to determine the magnetic field near the plasma both for the conductive and dielectric target.

[1] NASA demonstrates an idea for converting laser energy to electricity in satellites, Laser Focus **13**, 20 (1977).
[2] V. V. Korobkin and S. L. Motylev, Pis'ma Zh. Tekh. Fiz. **5**, 1135 (1979) [Sov. Tech. Phys. Lett. **5**, 474 (1979)].
[3] H. Daido, F. Miki, K. Mima, M. Fujita, K. Sawai, H. Fujita, Y. Kitagawa, S. Nakai, and C. Yamanaka, Phys. Rev. Lett. **56**, 846 (1986).
[4] H. Daido, K. Mima, F. Miki, M. Fujita, Y. Kitagawa, S. Nakai, and C. Yamanaka, Jpn. J. Appl. Phys. **26**, 1290 (1987).
[5] J. A. Stamper and B. H. Ripin, Phys. Rev. Lett. **34**, 138 (1975).
[6] J. A. Stamper, K. Papadopoulos, R. N. Sudan, S. O. Dean, E. A. McLean, and J. M. Dawson, Phys. Rev. Lett. **26**, 1012 (1971).
[7] G. Dimonte and L. G. Wiley, Phys. Rev. Lett. **67**, 1755 (1991).
[8] V. V. Korobkin and R. V. Serov, Pis'ma Zh. Eksp. Teor. Fiz. **4**, 103 (1966) [JETP Lett. **4**, 70 (1966)].
[9] G. A. Askarjan, M. S. Rabinovich, A. D. Smirnova, and V. B. Studenov, Pis'ma Zh. Eksp. Teor. Fiz. **5**, 116 (1967) [JETP Lett. **5**, 93 (1967)].
[10] V. V. Korobkin and S. L. Motylev, Pis'ma Zh. Eksp. Teor. Fiz. **29**, 700 (1979) [JETP Lett. **29**, 643 (1979)].
[11] A. V. Kabashin, V. I. Konov, P. I. Nikitin, A. M. Prokhorov,

N. Konjevic, and L. Vikor, J. Appl. Phys. **68**, 3140 (1990).
[12] A. V. Kabashin and P. I. Nikitin, Appl. Phys. Lett. **68**, 173 (1996).
[13] D. A. Aksionov, V. I. Konov, P. I. Nikitin, A. M. Prokhorov, A. I. Savchuk, A. V. Savitsky, and K. S. Ulyanitsky, Sensors Actuators **A23**, 875 (1990).
[14] S. N. Baribin, A. N. Grigorenko, V. I. Konov, and P. I. Nikitin, Sensors and Actuators, **A25-27**, 767 (1991).
[15] V. I. Konov, P. I. Nikitin, A. M. Prokhorov, and A. S. Silenok, Pis'ma Zh. Eksp. Teor. Fiz. **39**, 501 (1984) [JETP Lett. **39**, 609 (1984)].
[16] V. I. Konov, P. I. Nikitin, and A. M. Prokhorov, Izv. Acad. Nauk SSSR, Ser. Fiz. **49**, 1208 (1985) [Bull. Acad. Sci. USSR Phys. Ser. **48**, 159 (1985)].
[17] S. R. Case, Jr. and F. Schwirzke, J. Appl. Phys. **46**, 1493 (1975).
[18] P. F. Edwards, V. V. Korobkin, S. L. Motylev, and R. V. Serov, Phys. Rev. A **16**, 2437 (1977).